PRAMANA
— journal of
physics

© Printed in India

Vol. 44, No. 6,
June 1995
pp. 555–562

Collision cross-sections for scattering of electrons from NO molecule

ARVIND KUMAR JAIN, PRADEEP KUMAR and A N TRIPATHI
Department of Physics, University of Roorkee, Roorkee 247 667, India

MS received 10 November 1994

Abstract. Electron–NO scattering is investigated in the energy range 2–1000 eV by using a parameter-free spherical complex optical potential (SCOP) approach in the fixed nuclei approximation. The real part of the optical potential consists of three potentials namely, the static, the exchange and the polarization. For the imaginary part of the SCOP, we employ a semi-empirical model absorption potential. The molecular charge density function is calculated from a single-configuration molecular orbital based on Slater type orbitals. The various potential terms are then determined from these charge density functions. Calculations of the elastic (with and without absorption effects), total absorption, momentum transfer and differential cross-sections are obtained and compared with the available theoretical results and experimental measurements.

Keywords. Electron; charge density; potential; scattering.

PACS Nos 34·80; 34·90; 52·20

1. Introduction

The electron scattering from NO molecules plays an important role in many applied sciences, for example its role in the catalytic destruction of ozone in atmospheric studies is very well known. There is a paucity of theoretical and experimental electron impact cross-section data for this molecule. The total cross-section measurements on the e–NO system are available due to [1–4]. The experimental elastic e–NO differential cross-sections (DCS) at low energies (5, 10 and 20 eV) were reported by Kubo *et al* [5]. However, recently Brunger *et al* [6] have also reported their experimental DCS at these energies. Electron transmission experiments have observed strong resonance features in the low energy e–NO scattering [7]. The resonance positions and width for e–NO scattering using R-matrix method has been calculated by Tennyson and Noble [8]. Very recently Lee *et al* [9] have also investigated the elastic DCS due to low energy electron impact using a Born-closure Schwinger variational method (BCSVM) and its variants.

It is a well known fact that low energy electron molecule scattering is very sensitive to the treatment of short-range correlation (electron exchange and relaxation of bound orbitals due to impinging electron) and long-range polarization effects. In a model potential approach, the non-local nature of exchange and polarization effect is approximated by local forms [10].

Further, it should be noted that for the evaluation of total cross-section (σ_t) the optical potential of the interacting system must be complex; the imaginary part of the complex potential (known as absorption potential) takes into account the flux going

into all possible inelastic channels, such as ionization, electronic excitation and dissociation etc. It is because of this reason, the complex optical potential approach has been found very successful for predicting σ_t in the intermediate and high energy region collisions. There are a few *ab initio* techniques (e.g. see [11, 12]) available where electron-molecule problems can be pursued at rigorous level. Nevertheless such methods are very difficult from the computational point of view. It is always desirable to look for simple, local and parameter-free models which yield reliable scattering parameter with respect to experimental or more accurate theoretical results.

In this paper, we calculate the various scattering parameters i.e. DCS, elastic cross-section (σ_{el}), absorption cross-section (σ_{abs}), total (elastic + inelastic) cross-section (σ_t), momentum transfer cross-section (σ_m) and elastic cross-section without absorption effects (σ'_{el}) for electron scattering from NO molecules using a parameter-free spherical complex model potential in the energy range of (2–1000 eV). In the next section we give a brief description of theoretical methodology, while § 3 presents a discussion of the results and concluding remarks.

2. Theoretical methodology

The ground-state electronic configuration of NO is $1\sigma^2 2\sigma^2 3\sigma^2 4\sigma^2 1\pi^2 5\sigma^2 2\pi, X^2\pi$. The SCF molecular wavefunction of NO is taken from the compilation of Cade and Huo [13]. All calculations are performed for the bond lengths fixed as the equilibrium value $R_{N-O} = 2{\cdot}1747 a_0$. Within the framework of the fixed-nuclei approximation, the interaction of the electron molecule system can be represented by a local optical potential, i.e.

$$V_{opt}(\mathbf{r}) = V_R(\mathbf{r}) + iV_{abs}(\mathbf{r}) \tag{1}$$

where V_R, the real part of the total interaction, consists of three spherical local interactions, i.e.

$$V_R(\mathbf{r}) = V_{st}(\mathbf{r}) + V_{ex}(\mathbf{r}) + V_{pol}(\mathbf{r}). \tag{2}$$

Here the static potential (V_{st}) is the average over the ground-state molecular charge distribution of the electrostatic interaction of the electron and molecule. The V_{pol} represents approximately the short-range correlation and long-range polarization effects, while V_{ex} term accounts for electron exchange interaction and V_{abs}, is the absorption potential. All the potential terms (V_{st}, V_{ex}, V_{pol} and V_{abs}) are functions of charge density. In order to generate the target charge density and static potential, we employ a near Hartree–Fock wavefunction in terms of Slater type orbitals as given by Cade and Huo [13] following the VLAM and ALAM codes as given by Schmid *et al* [14] and Morrison [15] respectively. For example, the static potential in terms of legendre projections, v_λ, is given as

$$V_{st}(\mathbf{r}) = \sum_{\lambda=0}^{\lambda_{max}} v_\lambda^{st}(\mathbf{r})\, P_\lambda(\cos\theta). \tag{3}$$

We have taken about $\lambda_{max} = 20$ and 40 for electronic and nuclear contributions, respectively, in the expansion of the static potential. The static potential (V_{st}) is augmented by a parameter-free model of correlation polarization interactions which

has a simple dependence of charge density and polarizability (see [16, 17]. For the present calculation, the value of dipole polarizability is taken as 11·47 a.u. [18].

The exchange effect is incorporated through the Hara free electron gas exchange (HFEGE) [19] and modified semi-classical exchange (MSCE) [20]. The V_{abs} in (1) is the absorption potential which represents approximately the combined effect of all the inelastic channels. Here we employ a semi-empirical absorption potential as discussed by Staszewska *et al* [21]. The V_{abs} is the function of molecular charge density, incident electron energy and the mean excitation energy (Δ) of the target. Here we have taken Δ to be the ionization potential (I.P.) of the molecule. After generating the full optical potential eq. (1) of a given electron-molecule system, we treat it exactly in a partial wave analysis following a variable-phase-approach (VPA) (for details see, [10]). The various scattering parameters i.e. DCS, σ_{el}, σ_{abs}, σ_t, σ'_{el}, and σ_m are then easily obtained from the complex S-matrix at each energy.

3. Results and discussion

We have calculated several models with and without absorption potential. They are abbreviated as follows: S, pure static only; SH, S plus HFEGE potential; SHP, SH plus the correlation polarization potential; SE, S plus MSCE potential; SEP, SE plus the correlation polarization potential; and SHPa, SHP plus the absorption potential. Figures 1–4 show our DCS at 20, 30, 100 and 200 eV. In figures 1 and 2 we have shown our DCS in SHPa, SHP and SEP models at 20 and 30 eV, respectively, alongwith the measurements of Brunger *et al* [6] and Kubo *et al* [5]. We have also shown the results of recent calculations of Lee *et al* [9] using both BCSVM and SVIM approaches. It is seen that the present results of both models SEP and SHP yield similar DCS in the

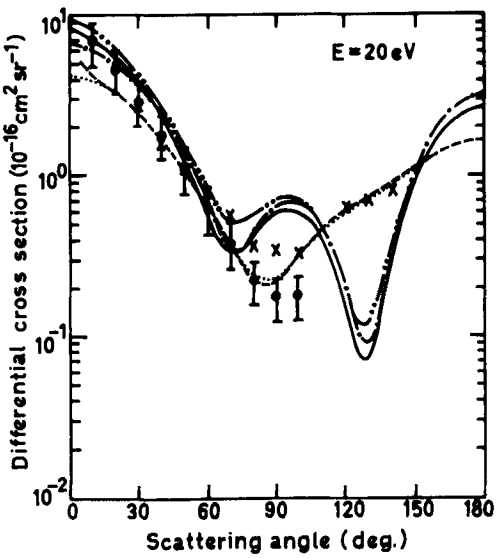

Figure 1. Differential cross-sections for e–NO scattering at 20 eV. Present calculations: ——, SHPa model; —•—, SHP model; —••—, SEP model (for notations see text); – – –, theoretical BCSVM results of Lee *et al* [9]; ....., theoretical SVIM results of Lee *et al* [9]. Experimental data: ⊕, Brunger *et al* [6]; ×, Kubo *et al* [5].

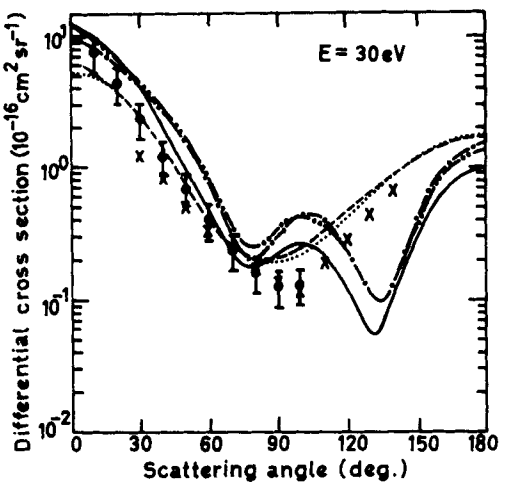

Figure 2. Same legend as in figure 2 except at 30 eV.

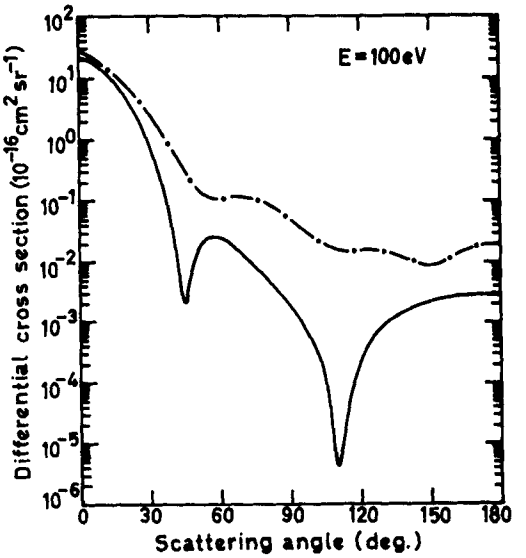

Figure 3. Differential cross-sections for e–NO scattering at 100 eV. Present calculations: ——, SHPa model; — • —, SHP model (for notations see text).

entire angular region, both giving the forward peak ($\theta < 20°$) compared to the S model and therefore we have displayed our results only in the SHP model in subsequent figures 3 and 4. Further, we also see that the results in SHPa model exhibit the forward peaking and are similar in shape to the results in SHP model in the entire angular region.

At these energies of 20 eV and 30 eV, the new measurements due to Brunger *et al* [6] are available at smaller scattering angles i.e. in the range of 5° to 100° whereas Kubo *et al*'s are in the range of 30° to 140°. At lower angles $\theta < 40°$, we find a good quantitative

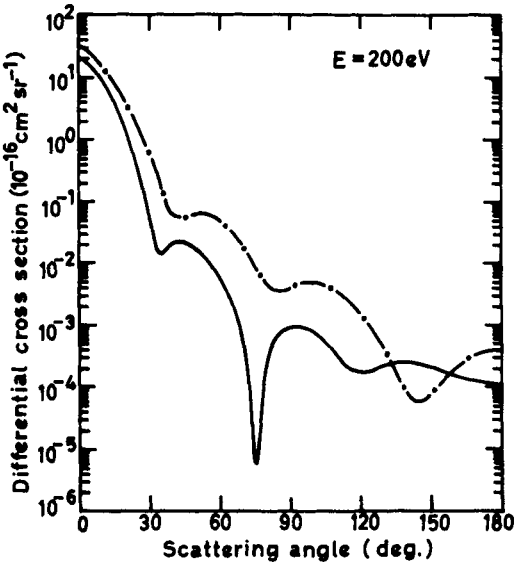

Figure 4. Same legend as in figure 3 except at 200 eV.

agreement between our theory and the data of Brunger *et al* [6]. Further, we see here that the DCS curves in SHPa model compare better with the measured results relative to the corresponding DCS in SHP model. The calculation of Lee *et al* [9] underestimates the cross-section almost by a factor of two at these angles. The disagreement between our results and the calculation of Lee *et al* [9] is probably due to neglect of polarization effects. Tennyson and Noble [8] have also observed that the inclusion of polarization is quite important for low energy elastic scattering for such molecules. Further, the present DCS exhibit dips around 65° and 130° accompanied by a shallow peak at 90° in between the two dips and thereafter, it shows a large backward peaking at large scattering angles, whereas the calculated results of Lee *et al* [9] reproduce the position of dip better compared to the present calculations as observed in the measurements. It is also to be noted that the measurements of Bruger *et al* [6] and Kubo *et al* [5] differ in the magnitude of cross-section values and the position of the dip. These variations in the angular distribution with respect to the experiment and theory narrow down with the increase in the impact energy (see figure 2). In figures 3 and 4, we show our calculated DCS for incident energies 100 and 200 eV only in SHPa and SHP models. At these higher energies, the DCS curves in SHPa model are rich in structure, in particular, the structure of dips and humps, both in magnitude and width, and change significantly relative to the DCS in SHP model. These oscillations show the typical characteristic of electron diffraction in the calculated DCS, a similar feature is also noticed in the recent calculation of Lee *et al* [9].

Finally, in figures 5 and 6, we have plotted our total (σ_t) and momentum transfer cross-sections (σ_m) in SHPa, SHP and SEP models in the energy regime (2–1000 eV) respectively. The results for the corresponding σ_t in this energy region is also compiled in table 1. For comparison, we have also displayed on the curve, the recent available experimental measurements of Szmytkowski and Maciag [4] in the energy region (1–160 eV). The important feature of the experimental result is an oscillatory structure at an incident energy below 2 eV and a broad hump with a maximum close to 16 eV.

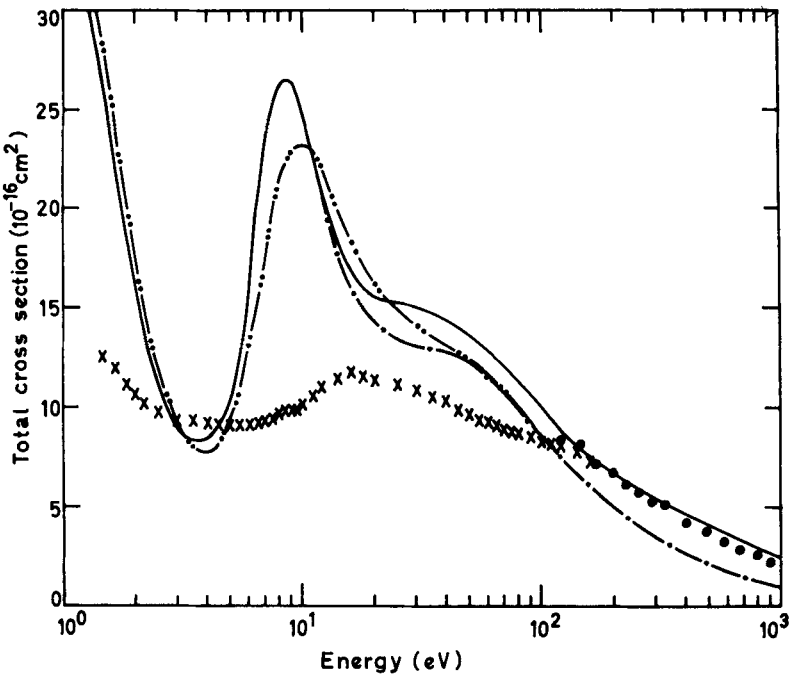

Figure 5. Total cross-sections for e–NO scattering as a function of electron energy, Present calculations: ——, SHPa model; —•—, SHP model; —••—, SEP model (for notations see text); Experimental data: ×, Szmytkowski and Maciag [4]; ●, Dalba *et al* [2].

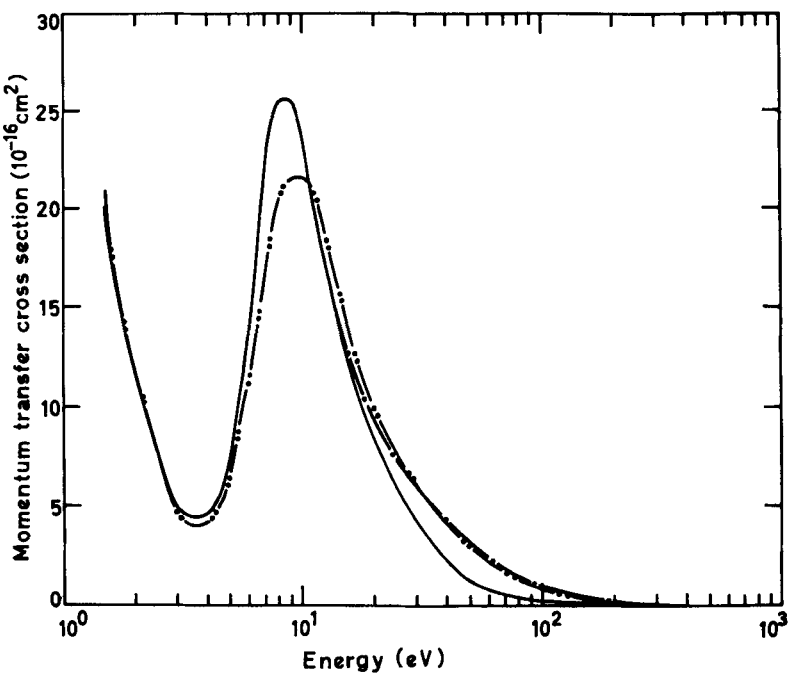

Figure 6. Momentum transfer cross-sections for e–NO scattering as a function of electron energy. Present calculations: ——, SHPa model; —•—, SHP model; —••—, SEP model (for notations see text).

Table 1. Elastic (σ_{el}), absorption (σ_{abs}), and total (σ_t) cross-sections in units of 10^{-16} cm^2 in SHP model with absorption effects. σ'_{el} is the elastic scattering cross-section without absorption effects (for notations see text).

Energy (eV)	σ'_{el}	σ_{el}	σ_{abs}	σ_t	Expt. Szmytkowski and Maciag [4]
2·00	16·59	16·59	0·00	16·59	10·7
5·00	10·81	10·81	0·00	10·81	9·22
10·00	24·80	24·80	0·01	24·81	10·1
20·00	14·29	13·79	1·74	15·53	11·4
30·00	13·25	11·69	3·54	15·23	10·8
40·00	12·90	10·33	4·55	14·88	10·3
50·00	12·40	9·10	5·04	14·14	9·59
60·00	11·70	7·95	5·25	13·20	9·30
70·00	10·91	6·98	5·29	12·27	8·96
80·00	10·14	6·27	5·21	11·48	8·75
90·00	9·43	9·53	5·15	10·68	8·58
100·00	8·79	5·22	4·97	10·19	8·48
110·00	8·23	4·51	4·94	9·45	8·29
120·00	7·72	4·05	4·85	8·90	8·13
140·00	6·86	3·45	4·63	8·08	7·76
160·00	6·16	2·99	4·43	7·42	7·44
200·00	5·09	2·62	4·04	6·66	—
300·00	3·52	2·18	3·35	5·53	—
400·00	2·68	1·87	2·89	4·76	—
500·00	2·16	1·63	2·54	4·17	—
700·00	1·55	1·28	2·05	3·33	—
1000·00	1·09	0·99	1·59	2·58	—

Further, the experimental results available from other groups [3] are in good accord with respect to the position of maxima near the oscillatory structure but they all differ with the recent measurements of Szmytkowski and Maciag (SM) [4]. The calculated values in the present models SHP and SEP exhibit almost similar variation with the maximum centred around 10 eV which is at lower energies compared to experimental measurements (around 16 eV). Our calculated results are higher by a factor of two compared to the recent available data of SM. The disagreement between our results and the experimental data with respect to magnitude of the cross-section values around 2 eV is consistent with earlier calculations in the e–CO scattering [22]. For energies above 100 eV, a comparison for the total cross-section is presented with the measured values of Dalba *et al* [2]. Our values in SHP model are smaller by 40% than those of Dalba *et al* [2]. On the contrary, the results of SHPa model show a very good agreement with the measured values of Dalba *et al* [2]. It clearly shows that the agreement with the experimental data with the inclusion of absorption effect in the calculation is better than the usual calculation without absorption effects at higher impact energies where inelastic channels become important. Figure 6 shows our σ_m cross-sections in the same energy region, where the shape of the cross-section is very similar to the σ_t curve of figure 5. To the best of our knowledge, no theoretical or experimental data are available in the literature for comparison of σ_m values.

We have presented differential, elastic (with and without absorption effects), total and momentum transfer cross-sections for electron scattering from NO molecule in the energy range of 2–1000 eV. A parameter-free spherical complex optical potential is treated exactly in the partial wave scheme to obtain the various scattering parameters. Various choices of exchange, a parameter-free correlation polarization and static potentials are derived from the *ab initio* molecular charge density. The inclusion of absorption effects is important at higher impact energies. All the salient features in the cross-sections, observed in various measurements for both the differential and total cross-sections are reproduced well by the present theoretical model.

Acknowledgement

This research is funded by the Department of Science and Technology, New Delhi, India under the project No. SR/SY/P-16/90.

References

[1] E Bruche, *Ann. Phys. Lpz.* **83**, 1065 (1927)
[2] G Dalba, P Fornasini, R Grisenti, G Ranieri and A Zecca *J. Phys.* **B13**, 4695 (1980)
[3] A Zecca, I Lazzizzera, M Krauss and C E Kuyatt, *J. Chem. Phys.* **61**, 4560 (1974)
[4] C Szmytkowski and K Maciag, *J. Phys.* **B24**, 4273 (1991)
[5] M Kubo, D Matsunaga, T Suzuki and H Tanaka *Proc. 12th Int. Conf. on the Phys. of Electronic and Atomic Collisions (Gatlinburg)* (North-Holland, Amsterdam, 1981) p. 360
[6] M J Brunger *et al* (1993) *Private communication to the author*
[7] M Tronc, G C King and F H Read, *J. Phys.* **B13**, 999 (1980)
[8] J Tennyson and C J Noble, *J. Phys.* **B19**, 4025 (1986)
[9] M-T Lee, M Fujimoto, S E Michelin, L E Machado and L M Brescansin, *J. Phys.* **B25**, L505 (1992)
[10] A Jain and K L Baluja, *Phys. Rev.* **A45**, 202 (1992)
[11] P G Burke and J B West eds. *Electron molecule scattering and photoionization* (Plenum: New York, 1987)
[12] A Herzenburg, *Aspects of electron–molecule scattering and photoionization* (AIP: New York, 1990)
[13] P E Cade and W M Huo, *At. Data Nucl. Data Tables* **15**, 2 (1975)
[14] G B Schmid, D W Norcross and L A Collins *Comput. Phys. Commun.* **21**, 79 (1980)
[15] M A Morrison, *Comput. Phys. Commun.* **21**, 63 (1980)
[16] N T Padial and D W Norcross, *Phys. Rev.* **A29**, 15 (1984)
[17] F A Gianturco, A Jain and L C Pantano, *J. Phys.* **B20**, 571 (1987)
[18] T M Miller, *CRC Handbook of Chemistry and Physics* (Boca Raton F L, Chemical Rubber, 1984)
[19] S Hara, *J. Phys. Soc. Jpn.* **22**, 710 (1967)
[20] F A Gianturco and S Scialla, *J. Phys.* **B20**, 3171 (1987)
[21] G Staszewska, D W Schwenke and D G Truhlar, *Phys. Rev.* **A29**, 3078 (1984)
[22] A Jain and D W Norcross, *Phys. Rev.* **A45**, 1644 (1992)